Title	A model code for the radiative theta pinch
Author(s)	S. Lee, S. H. Saw, P. C. K. Lee, M. Akel, V. Damideh, N. A. D. Khattak, R. Mongkolnavin and B. Paosawatyanyong
Source	*Physics of Plasmas, 21*(7): 072501; doi: 10.1063/1.4886359
Published by	American Institute of Physics

A model code for the radiative theta pinch

S. Lee,[1,2,3,a)] S. H. Saw,[1,2] P. C. K. Lee,[4] M. Akel,[5] V. Damideh,[1] N. A. D. Khattak,[6] R. Mongkolnavin,[7] and B. Paosawatyanyong[7]
[1]*INTI International University, 71800 Nilai, Malaysia*
[2]*Institute for Plasma Focus Studies, 32 Oakpark Drive, Chadstone 3148 Australia*
[3]*Physics Department, University of Malaya, Kuala Lumpur, Malaysia*
[4]*Nanyang Technological University, National Institute of Education, Singapore 637616*
[5]*Department of Physics, Atomic Energy Commission, Damascus, P. O. Box 6091, Damascus, Syria*
[6]*Department of Physics, Gomal University, Dera Ismail Khan, Pakistan*
[7]*Department of Physics, Faculty of Science, Chulalongkorn University, Bangkok 10140, Thailand*

(Received 5 May 2014; accepted 20 June 2014; published online 3 July 2014)

A model for the theta pinch is presented with three modelled phases of radial inward shock phase, reflected shock phase, and a final pinch phase. The governing equations for the phases are derived incorporating thermodynamics and radiation and radiation-coupled dynamics in the pinch phase. A code is written incorporating correction for the effects of transit delay of small disturbing speeds and the effects of plasma self-absorption on the radiation. Two model parameters are incorporated into the model, the coupling coefficient f between the primary loop current and the induced plasma current and the mass swept up factor f_m. These values are taken from experiments carried out in the Chulalongkorn theta pinch. © *2014 AIP Publishing LLC*. [http://dx.doi.org/10.1063/1.4886359]

I. INTRODUCTION

A theta pinch may use a single conducting wide-loop of capacitor-pulsed current wrapped around a cylindrical glass tube containing a gas at low pressure.[1,2] The pulsed magnetic field associated with this primary current I_c generates a potential which breaks down the gas in the tube and drives a current in the tube. The induced current loop heats the gas producing plasma. Initial ionization is likely to be produced on the inner surface of the glass tube. Hence, we take the starting radius of the plasma current loop as the radius of the glass tube.

This current I_{plasma} flows in an opposite direction to the primary (circuit current I_c, shown schematically in Fig. 1; cross-section shown schematically in Fig. 2). With a large enough current, the electromagnetic force operating between these two opposing current loops drives the plasma current loop radially inwards producing a pinched column of plasma on the axis of the tube.

Since the plasma current is pushed radially inwards, the plasma forming the pinch is not in contact with any electrode and is hence cleaner than either the Z-pinch or the plasma focus. This is a particularly useful feature for using the plasma pinch as a light source for spectroscopic purposes.[2]

II. THE MODEL

The Lee Model code[3,4] has been developed and successfully used to describe a capacitor current directly driving the axial phase followed by radial phases of a plasma focus. This paper adapts the radial phases of that Model code to describe the theta pinch. In the radial phase of the plasma focus, the driving current flows in the axial direction along a cylinder, producing an azimuthal magnetic field which compresses the plasma cylinder.[3,4] This is different from the azimuthal currents of the theta pinch which produces axial fields (see Fig. 2). In the theta pinch, the driving force may be quantified by the difference of the magnetic pressure exerted by the axial magnetic field of the primary fixed circuit loop minus the magnetic pressure exerted by the axial magnetic field of the secondary moving plasma loop. To adapt the plasma focus radial phase code to the theta pinch, the above points are incorporated. Another major difference for the theta pinch model is the circuit equation which needs to couple the discharge current in the primary loop to the plasma current flowing in the secondary plasma loop. The plasma loop interacts with the primary loop, with a repulsive force causing the plasma current sheet to be driven radially inwards pushing a cylindrical layer (or slug) ahead of it (see Fig. 2, see also Fig. 3 which is a radius vs time schematic of the compression).

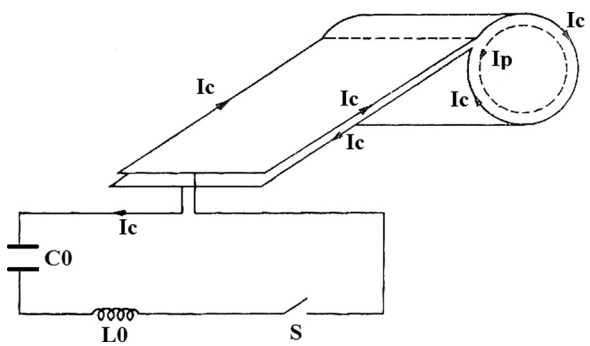

FIG. 1. Schematic of theta pinch showing primary current I_c and induced plasma current I_p (glass tube not shown). The parallel plate strip-line connects the capacitor bank C_0 to the primary coil and is shown with the same width as the primary coil (width l_c not labelled). The spark-gap switch is depicted by S. High voltage insulation and the stray circuit resistance r_0 are not shown in the schematic.

a)e-mail: leesing@optusnet.com.au

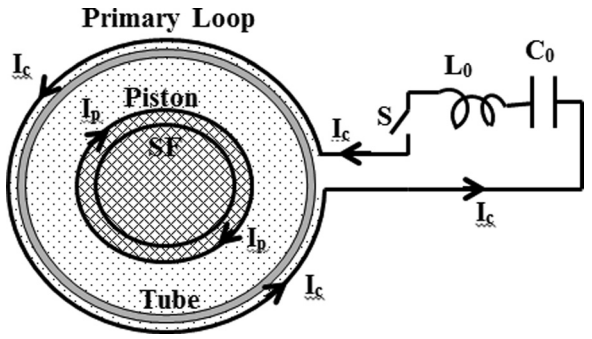

FIG. 2. Showing the x-section of the theta pinch with primary current coil (width l_c) carrying circuit current I_c wrapped around the outside of the glass tube and induced plasma current I_p in the low pressure gas in the glass tube. The induced current sheath acts as a magnetic piston—its interaction with the primary loop pushes the piston radially inwards (away from the glass tube inner wall). The motion is highly supersonic and drives a radial SF ahead of the piston. (The SF is not shown in Fig. 1.) The primary loop current I_c produces a magnetic field $B = \mu I_c/l_c$ pointing upwards out of the page in the area enclosed by the primary loop; whilst the induced current I_p (piston) produces a magnetic field $B = \mu I_p/l_c$ pointing into the page in the area enclosed by the induced current loop. The stray circuit resistance r_0 is not shown in the schematic.

A. Radial inward shock phase

The front of this layer is a radially converging shock (shock front, SF, in Figs. 2 and 3) at position r_s. Ahead of the shock (i.e., radius $< r_s$) is ambient gas. Between the SF and the magnetic piston (current sheath, CS) is the "slug" of shock heated plasma. The position of the piston is r_p. Behind r_p (i.e., radius $> r_p$) is a vacuum. All the gases encountered by the shock front are swept into the "slug," i.e., between radial positions r_s and r_p. Any imperfection in the sweeping mechanism is expressed by a factor f_m the fraction of mass swept up. The circuit equation contains an inductance term which is made up of the inductance of the primary coil moderated by the inductance of the secondary (plasma) coil. This provides the coupling of the plasma motion into the circuit equation. This concept is equivalent to the consideration of the interaction of the two inductances as a mutual inductance. The net magnetic pressure exerted by the two coils on the plasma slug drives the radial shock front in the inwards direction. This determines the trajectory of the radial shock. The piston position at any point of time is calculated from the shock position by using an adiabatic rule. Following the Lee Model code, in considering the relationship between the shock front position and the piston position, we also consider the effect of non-infinite small disturbance speed (SDS).[3–5]

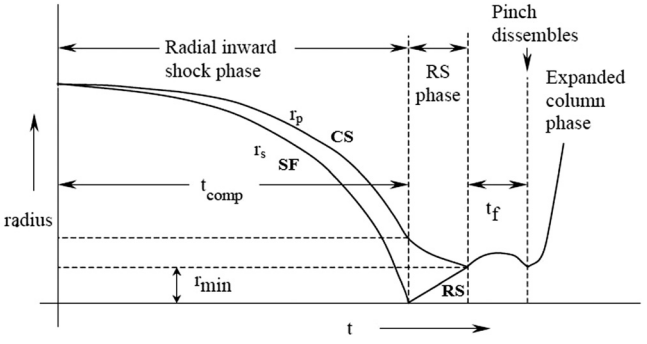

FIG. 3. Radius vs time schematic of the trajectories of the radial SF and radial CS.

The inward moving shock starts at position $r_s = r_c$ (whilst the piston starts at position $r_p = r_c$) and is driven inwards until the axis at position $r_s = 0$. We call this phase the inward shock phase or phase 1 of this model code.

B. Reflected shock (RS) phase

When the inward radial shock goes on axis (i.e., $r_s = 0$), provided the plasma is collisional as we assume, a RS develops, moving radially outwards; its position is assigned as r_{rs}. In front of the outwardly moving RS position r_{rs} (up to the region bounded by the inwardly moving magnetic piston at position r_p) is plasma already compressed and heated by the earlier passage of the inward moving shock. Behind r_{rs} is a region compressed and heated by the earlier passage of the inward moving shock and then further compressed and heated by the passage of the RS. This region, bounded by r_{rs} is a stagnated region (directed plasma motion reduced to zero), doubly shock-compressed and heated. This phase 2 (RS phase) ends when the outward going RS meets the incoming piston, i.e., when $r_{rs} = r_p$. The RS temperature is postulated to decrease as the RS moves outwards; referenced to the radially inward shock speed (which had been recorded) at each RS position.

C. Slow compression (pinch) phase

The end of phase 2 marks the start of phase 3, the slow compression or pinch phase characterized in dynamics by r_p, the position of the piston enveloping the plasma pinch. Typically, the experiment may be designed to still have sufficient driving current at this time so that the piston is still compressing strongly enough to "pinch" the plasma column further inwards. The end of this pinch phase 3, may have the column disrupted by instabilities.[6] Typically, this pinch phase is the one of interest in the applications of the theta pinch as a spectroscopic source. We include into this phase radiation equations for Bremsstrahlung, recombination, and line radiation, noting that for the range of operation of this device and for the gases used, typically argon or neon, line radiation is likely to dominate. We include plasma self-absorption to obtain a realistic radiation yield out of the pinch.[3,4,7,8] In this phase, we also include Joule heating. The net gain/loss of these powers is included into the piston motion equation so that the dynamics is thermodynamically and radiatively coupled. The duration of this phase (termed t_f in Fig. 3) may be computed by taking the transit time of small disturbances across the pinch column. The computation is stopped at the end of the pinch phase.

III. THE EQUATIONS OF THE MODEL

A. Phase 1: The inward shock phase

1. The circuit equation

A current I_c flowing around a long cylinder of length l_c produces an axial magnetic field or magnetic flux density

$B = \mu I_c/l_c$ T m^{-2}. If the cylinder radius is r_c, the magnetic flux $= \mu\pi {r_c}^2 I_c/l_c$ T.

The plasma current loop I_p produces magnetic flux $= \mu\pi {r_p}^2 I_p/l_c$ T, this flux being in opposite direction to the flux produced by I_c. Unless otherwise stated the units are in SI.

From Fig. 2, we note that the net flux encompassed by the primary loop is

$$\text{Flux} = \mu\pi r_c^2 I_c/l_c - \mu\pi r_p^2 I_p/l_c.$$

The flux produced per unit current I_c gives the inductance L_c perceived by the primary circuit

$$L_c = \mu\pi r_c^2/l_c - \mu\pi r_p^2 I_p/(I c l_c) \text{ or } L_c = (\mu\pi/l_c)(r_c^2 - f r_p^2),$$

where $f = I_p/I_c$ is the current coupling coefficient, assumed constant throughout the dynamics of the theta pinch. This assumption is consistent with the fitting of computed and measured current waveforms.[1]

We write the circuit equation as

$$\frac{d}{dt}[(L_o + (\mu\pi/l_c)(r_c^2 - f r_p^2))I_c] + r_o I_c = V_o - \int \frac{I_c dt}{C_o}.$$

This gives us the first generating equation for this phase

$$\frac{dI_c}{dt} = \left[V_o - \frac{\int I_c dt}{C_o} - r_o I_c + 2(\pi\mu/l_c) f r_p I_c \frac{dr_p}{dt}\right] \Big/ [L_o + (\pi\mu/l_c)(r_c^2 - f r_p^2)]. \quad (1)$$

2. The equations of motion

a. Shock speed. The magnetic pressure exerted by the magnetic piston $P_m = P_{mc} - P_{mp}$, where P_{mc} is the magnetic pressure behind the piston and P_{mp} is the magnetic pressure in front of the piston.

$$P_m = P_{mc} - P_{mp} = (\mu I_c/l_c)^2/2\mu - [\mu(I_c - I_p)/l_c]^2/2\mu = \mu f (I_c/l_c)^2 (2 - f)/2.$$

From shock wave theory,[9–12] the pressure behind the shock (travelling at speed dr_s/dt) is $P = (2/(\gamma+1))(f_m \rho_0)(drs/dt)^2$ where γ is the specific heat ratio of the plasma and $f_m\rho_0$ is the effective density of the shock moving into ambient density ρ_0 subjected to a swept up fraction of f_m. If we assume that this pressure is uniform from the SF to the CS (infinite acoustic small disturbance speed approximation) then across the piston, we may apply $P = P_m$ and thus obtain the equation of the shock speed

$$\frac{dr_s}{dt} = -\left[\frac{\mu(\gamma+1)}{4}\right]^{\frac{1}{2}} \left[\frac{f(2-f)}{f_m}\right]^{\frac{1}{2}} \frac{(Ic/lc)}{\sqrt{\rho_0}}. \quad (2)$$

b. Piston speed. The speed of the magnetic piston (CS) is determined by the first law of thermodynamics applied to the effective increase in volume between SF and CS,[5] created by incremental motion of the SF.[3–5,9,11] This consideration gives us the speed of the magnetic piston (CS)

$$\frac{dr_p}{dt} = \frac{\frac{2}{\gamma+1}\frac{r_s}{r_p}\frac{dr_s}{dt} - \frac{r_p}{\gamma Ic}\left(1 - \frac{r_s^2}{r_p^2}\right)\frac{dIc}{dt}}{\frac{\gamma-1}{\gamma} + \frac{1}{\gamma}\frac{r_s^2}{r_p^2}}. \quad (3)$$

Equations (1)–(3) are the generating equations of the system.

c. Normalisation of equations. For this phase, the following normalization is adopted in order to get the scaling parameters:

$\tau = t/t_0$, $\imath = I/I_0$ with $\kappa_s = r_s/r_c$, $\kappa_p = r_p/r_c$, i.e., distances are normalized to primary coil radius. The electrical characteristic quantities are: characteristic time $t_0 = (L_0 C_0)^{0.5}$ and characteristic current $I_0 = V_0/(L_0/C_0)^{0.5}$. We have

$$\textbf{Radial shock speed}: \quad \frac{d\kappa_s}{d\tau} = -\alpha\imath, \quad (4)$$

$$\textbf{Radial piston speed}: \quad \frac{d\kappa_p}{d\tau} = \frac{\frac{2}{\gamma+1}\frac{\kappa_s}{\kappa_p}\frac{d\kappa_s}{d\tau} - \frac{\kappa_p}{\gamma\imath}\left(1 - \frac{\kappa_s^2}{\kappa_p^2}\right)\frac{d\imath}{d\tau}}{((\gamma-1)/\gamma) + (1/\gamma)(\kappa_s^2/\kappa_p^2)}, \quad (5)$$

$$\textbf{Current rate}: \quad \frac{d\imath}{d\tau} = \frac{1 - \int \imath d\tau - \delta\imath + 2f\beta k p \imath \frac{d\kappa_p}{d\tau}}{\{1 + \beta - f\beta k p^2\}}, \quad (6)$$

where the **scaling parameters** are $\beta = (\pi\mu {r_c}^2/l_c)/L_0$ (ratio of primary coil inductance to L_0); $\delta = r_0/(L_0/C_0)^{0.5}$ (circuit damping factor), and $\alpha = t_0/t_s$ where t_s is the characteristic time of the inward shock phase and

$$t_s = \frac{2 f_m^{0.5} r_c}{[\mu(\gamma+1) f(2-f)]^{0.5}} \frac{\rho_0^{0.5}}{(I0/l_c)}$$

and characteristic speed of inward shock to reach axis is

$$v_s = r_c/t_s = \frac{[\mu(\gamma+1) f(2-f)]^{0.5}}{2 f_m^{0.5}} \frac{(I_0/l_c)}{\rho_0^{0.5}}.$$

Note that the radial characteristic speed has the dependence on drive factor[10] $S = (I_c/l_c)/\sqrt{\rho_0}$.

Equations (4)–(6) are the generating equations in normalized form. By the process of normalizing the generating equations, we have found the characteristic speed of the radial inward shock phase.

With a given set-up, we have the electrical parameters: L_0, C_0, and r_0; the geometrical parameters r_c and l_c (we assume that the radius of the coil is the same as the inner radius of the glass tube) and operating parameters charging voltage V_0 and gas type and pressure. With some assumptions on the coil-plasma coupling constant f and mass swept up factor f_m, the 3 generating equations (1)–(3) can be solved step-by-step with linear approximations connecting

the charge with the current and the current with the rate of change of current and similar linear approximations connecting the radial positions with the radial speeds. The solutions are the current I_c, and the radial positions r_s and r_p as functions of time. Alternatively the normalized scaling parameters may be determined from the real parameters and the 3 normalized generating equations (4)–(6) may be used to solve for the currents and radial positions.

In the slug model above, we assume that the pressure exerted by the magnetic piston (current I_p, position r_p) is instantaneously felt by the shock front (position r_s). Likewise the shock speed dr_s/dt is instantaneously felt by the piston (CS). This assumption of infinite SDS is implicit in Eqs. (2) and (3). To correct for the non-infinite speed, a delay equal to the transit time of small disturbance is included into the code so that interactive effects are realistically portrayed.

B. Phase 2: The radial reflected shock phase

When the inward radial shock hits the axis, $\kappa_s = 0$. Thus, in the computation, when $\kappa_s \leq 1$, we exit from radial inward shock phase. We start computing the RS phase. The RS is given a constant speed of 0.3 of on-axis inward radial shock speed[3,4,12]

$$\textbf{Reflected shock speed}: \quad \frac{dr_r}{dt} = -0.3\left(\frac{dr_s}{dt}\right)_{on-axis}, \tag{7}$$

$$\textbf{Piston speed}: \quad \frac{dr_p}{dt} = \frac{-\frac{r_p}{\gamma Ic}\frac{dIc}{dt}}{\frac{\gamma-1}{\gamma}}. \tag{8}$$

Circuit equation: The circuit equation remains unchanged from that of phase 1.

Equations (7), (8), and (1) are the 3 generating equations for this RS phase 2. These 3 coupled equations are solved for the 3 unknowns I_c, r_s, r_p; using linear approximations to connect r_s to dr_s/dt, r_p to dr_p/dt, and dI_c/dt to I_c and to integral of I_c.

In this phase, the RS (position r_{rs}) moves outwards, the piston (position r_p) moves inwards. Eventually, the increasing value of r_{rs} reaches the decreasing value of r_p. The pinch phase starts.

C. Phase 3: Slow compression or pinch phase

In this phase, the piston speed is[3,4]

$$\frac{dr_p}{dt} = \frac{\frac{-r_p}{\gamma I}\frac{dI}{dt} + \frac{4\pi(\gamma-1)}{\mu\gamma l_c}\frac{r_p}{f^2 I_c^2}\frac{dQ}{dt}}{\frac{\gamma-1}{\gamma}} \tag{9}$$

and the circuit current equation is unchanged from Eq. (1).

Equations (1) and (9) are the generating equations for this pinch phase 3. These are solved step-by-step for I_c and r_p.

We have included the net energy loss/gain term dQ/dt into the equation of motion.[3,4]

The plasma gains energy from Joule heating and loses energy through Bremsstrahlung, recombination, and line radiation. Energy gain in the pinch will tend to push the piston outwards, whilst energy loss from the pinch will tend to compress the pinch further.

The Joule term is calculated from the following (plasma resistance R following Spitzer[13] and plasma temperature T following the Bennett equation[14]):

$$\frac{dQ_J}{dt} = RI_c^2 f^2 \quad R = \frac{1290 Z l_c}{\pi r_p^2 T^{\frac{3}{2}}},$$

$$T = \frac{\mu}{8\pi^2 k} I_c^2 f^2 / (D N_o r_c^2 f_m).$$

The Bremsstrahlung loss term may be written as[3,4]

$$\frac{dQ_B}{dt} = -1.6 \times 10^{-40} N_i^2 (\pi r_p^2) l_c T^{\frac{1}{2}} Z^3,$$

$$N_o = 6 \times 10^{26} \frac{\rho_o}{M}; \quad N_i = N_o f_m \left(\frac{r_c}{r_p}\right)^2.$$

The line loss term may be written as

$$\frac{dQ_L}{dt} = -4.6 \times 10^{-31} N_i^2 Z Z_n^4 (\pi r_p^2) l_c / T$$

$$\text{and } \frac{dQ}{dt} = \frac{dQ_J}{dt} + \frac{dQ_B}{dt} + \frac{dQ_L}{dt},$$

where dQ/dt is the total (net) power gain/loss of the plasma column.

By this coupling, if, for example, the radiation loss $dQ_B/dt + dQ_L/dt$ is severe, this would lead to a large value of dr_p/dt inwards. Radiation from the plasma causes the plasma to cool. This reduces its hydrostatic pressure. The constricting magnetic pressure is undiminished by the radiation. Thus, the compression is enhanced by radiative cooling. The more the radiation the greater is the imbalance between the constricting magnetic pressure and the greatly reduced hydrostatic pressure. This increases the speed of compression. In the extreme case, this radiative cooling leads to radiation collapse, with r_p going rapidly to zero, or to such small values that the plasma becomes opaque to the outgoing radiation, thus stopping the radiation loss.

This radiation collapse occurs at a critical current of 1.6 MA (the Pease-Braginski current[15,16]) for deuterium. For gases, such as Neon or Argon, because of intense line radiation, the critical current is reduced[17,18] to even below 100 kA, depending on the plasma temperature.

D. Plasma self absorption and transition from volumetric emission to surface emission

Plasma self-absorption and transition from volumetric emission (described above) to surface emission of the pinch column are implemented in the following manner.[3,4]

The photonic excitation number[8] is written as follows:

$$M = 1.66 \times 10^{-15} r_p Z_n^{0.5} n_i / (Z T^{1.5})$$

with T in eV, rest in SI units.

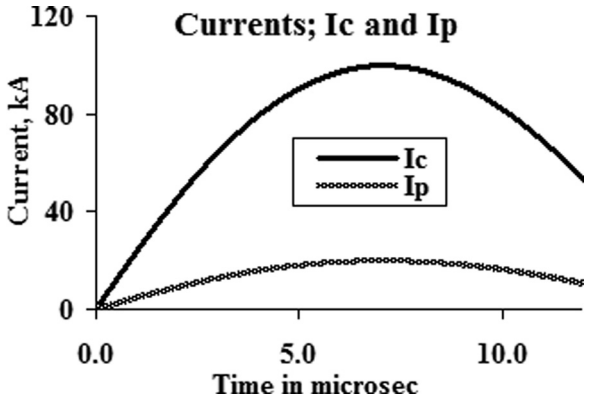

FIG. 4. Computed primary coil current I_c and induced plasma current I_p.

The volumetric plasma self-absorption correction factor A is obtained[8]

$$A_1 = (1 + 10^{-14} n_i Z)/(T^{3.5})); \; A_2 = 1 / A_{1;} A = A_2^{(1+M)}.$$

Transition from volumetric to surface emission occurs when A goes from 1 (no absorption) down to 1/e (e = 2.718) when the emission becomes surface-like given by the expression[8]

$$\frac{dQ_L}{dt} = -const Z^{0.5} Z_n^{3.5} r_p l_c T^4,$$

where const is taken as 4.62×10^{-16} to conform with numerical experimental observations that this value enables the smoothest transition, in general, from volumetric to surface emission.

IV. APPLYING THE RADIATIVE THETA PINCH CODE

Based on the above phases and equations the code is written for the 3 phases radially inwards shock, radially outward reflected shock, and slow compression (pinch). This code (phase 1 only) had been used by Chaisombata *et al.*[1] to describe the Chulalongkorn Pulsed Inductively Coupled Plasma (PICP) which is a theta pinch of the type described by this model. They measured a current (I_c) waveform from their device. They used phase 1 of the code described in this paper and fitted the computed current (I_c) waveform to this measured current using the current coupling factor f and the mass swept-up factor f_m as fitting parameters. At 9 kV, 10 Pa (0.08 Torr) in argon, they obtained f = 0.2 and fm = 0.78. Using a magnetic probe at 3 positions they obtained reasonable comparison of the measured current sheath trajectory versus the computed trajectory of the magnetic piston. In 1 case (12 kV 0.02 Torr), they also measured radial speed of 2.5 cm/μs with electron temperature of 3.9 eV (measured with optical emission spectroscopy).

To simulate the Chulalongkorn PICP, we configure a theta pinch using their parameters:

Bank parameters: $L_0 = 338$ nH, $C_0 = 60$ μF, $r_0 = 13$ mΩ,

Tube parameters: b = 5 .5 cm, a = 30 cm

Operating parameters: $V_0 = 9$ kV, $P_0 = 0$ .08 Torr argon

Model parameters: $f_m = 0$ .78, f = 0.2 (experimentally found[1]).

The results are shown in Figures 4–9.

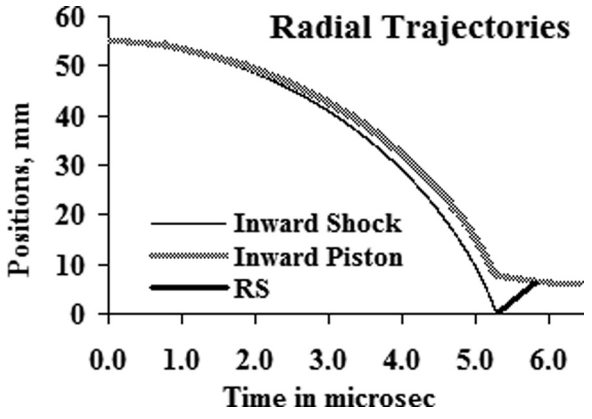

FIG. 5. Computed trajectories of radial inward-moving shock, radial outward-moving reflected shock, and the magnetic piston.

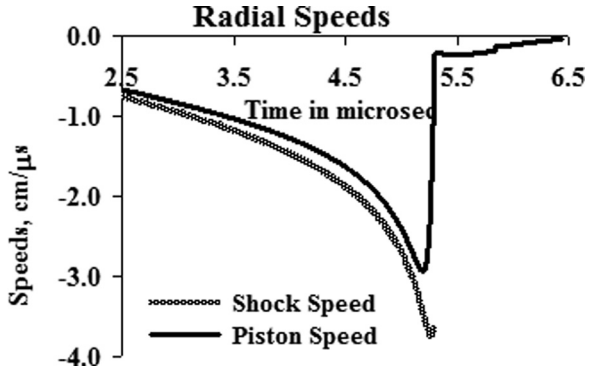

FIG. 6. Radial speeds of inward shock front and the magnetic piston between the times 2.5–6.5 μs.

V. RESULTS AND DISCUSSION

Figure 4 shows the computed primary coil current I_c and the plasma current I_p. The computed primary current waveform and peak value agree with those published in the Chulalongkorn paper.[1] The poor coupling constant of f = 0.2 derived in those experiments is responsible for the low plasma current I_p with a peak value of barely 20 kA.

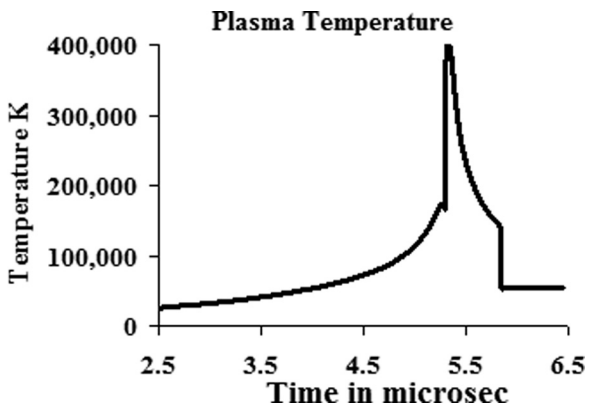

FIG. 7. Plasma temperature as a function of time between t = 2.5 and 6.5 μs.

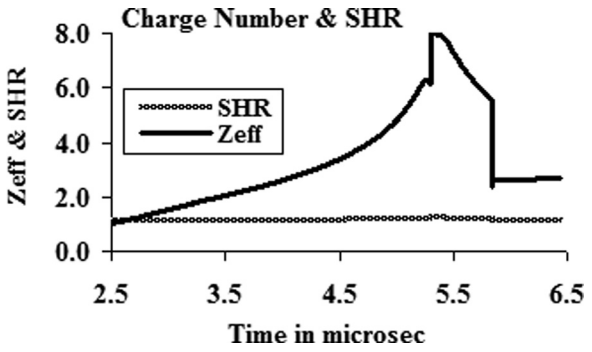

FIG. 8. Effective charge number Z and specific heat ratio SHR as functions of time.

Figure 5 shows the computed trajectory of the radially converging shock wave driven by the radially compressing piston. When the radial shock wave coalesces on the axis, a RS is formed, moving radially outwards. At the point when the radial shock wave collapses on-axis (about 5.3 μs), the piston is seen to decelerate sharply due to the physics[3–5] built into Eq. (3). The piston then continues moving slowly inwards whilst the RS moves radially outwards. They meet at 5.8 μs at which point the pinch is formed with the magnetic field surrounding the column of doubly shock heated gas. The current is still rising. For this situation, the pinched plasma column continues to be compressed slowly inwards by the magnetic field until the calculation is completed at 6.5 μs. It is noted that the computed trajectory of the magnetic piston (current sheet) agrees well with the experimental results of measured plasma current trajectory of the Chulalongkorn PICP.[1]

Figure 6 shows the speeds of the shock front and magnetic piston, shown with negative values indicating that the motions are radially inwards. The small values of piston speed between the times 5.3 and 5.8 μs show the sharp reduction in piston speeds during the RS phase. The very small but non-zero values of speeds from 5.8 until nearly 6.5 μs show the slow compression (or pinch) phase. RS speed is not shown in this figure.

Figure 7 shows the computed temperature time profile. For the radially inward shock phase, the inward shock speed determines the temperature which is seen to rise from 27 000 K at t = 2.5 μs reaching a value of 165 000 at 5.3 μs as the shock speed rises from 0.7 to 3.6 cm/μs; the dependence of temperature on shock speed squared being severely moderated by the increasing ionization levels of the argon plasma[3–5] from an effective charge number of 1.1–6.2 (see Fig. 8). When the fast moving shocked particles stagnate on-axis the RS temperature jumps to almost 400 000 K. As the RS moves radially outwards, the RS temperature is postulated to decrease based on the decreasing speed of the plasma stream encountered by the RS. In this modelling, the RS temperature drops from 385 000 K to 140 000 K by the time the outwardly moving RS meets the slowly incoming piston, defining the start of the pinch phase at t = 5.8 μs.

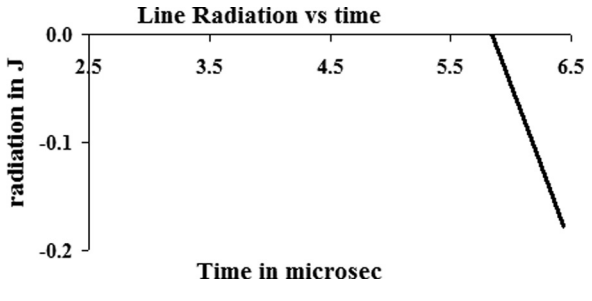

FIG. 9. Argon line radiation versus time.

At the start of the pinch, the drop of temperature from 140 000 K to 53 000 K may not be realistic, being due to mismatch of the two ways of calculating temperatures—before the start of pinch, temperature is based on RS modelling; after the start of pinch, temperature calculation is based on Bennett equation balancing pinch kinetic pressure with confining magnetic pressure.

The code calculates the effective charge number Z based on the ionization fractions as a function of temperature calculated using a corona model.[19] The specific heat ratio SHR is also calculated.[20] These thermodynamic quantities are required for the equations of the code, e.g., Eqs. (2) and (3). The data are stored in a set of fitted polynomials of temperature for input into the code whenever needed. In the time interval between t = 2.5 μs and 6.5 μs, the SHR has a value just under 1.2. The charge number Z rises from 1.1 at 2.5 μs to 6.2 as shock goes on-axis, then jumps to closed sub-shell value of 8 on formation of the RS on axis; then gradually falls to 5.6 as the RS temperature drops. With the formation of the pinch the value of Z has dropped to 2.6 before rising gradually to 2.7 towards the end of the pinch phase.

The argon line radiation is shown in Figure 9. As modelled, the line yield only becomes appreciable during the pinch phase, reaching a value of 0.17 J at the end of the pinch. We discuss the yield further in Sec. VI.

We discuss the results of our computation of plasma temperature in the light of the time-integrated measurement of electron temperature reported in the Chulalongkorn PICP.[1] Why is the high temperature we compute from 4.5 μs to 5.8 μs not observed in the PICP spectroscopic measurements?

We first note that with the plasma parameters we expect the electron temperature to be in equilibrium with the plasma temperature; in which case the electron temperature that is measured should also be the plasma temperature. Two factors in this situation need to be pointed out: The contribution to the observed time integrated optical intensity depends first on a factor which is essentially the integral of plasma density squared × volume × time. In the case of the inward shock phase, the volume of plasma is small and the density is small; and the value of this factor is small relative to that of the pinch phase. In the case of the RS phase, we have considered this factor which turns out to be less than 10% of that of the pinch phase. Thus, this factor determines that the observed optical intensity heavily favours observation of the pinch phase. The other factor to consider is the relative intensity of the lines available to the Chulalongkorn experimental setup of 200–800 nm. An inspection of the relative intensities of the lines within this spectral range[21,22] for Ar ions from first ionized Ar II to Ar IX shows that the lines recorded in the Chulalongkorn experiments are likely from Ar II to IV. This is consistent with the spectral contribution coming from the pinch which has effective charge number of 2.6. This is

confirmed by a careful study of NIST tables and line identification plots.[22]

Combining both the factors discussed above, observation based on spectral window of 200–800 nm will record only the pinch phase. Thus, our computed temperature of the pinch of 53 000 K is not too far away from the higher end of the measured range of 50 000 K of the PCIP experiment.[1] We note that Fig. 9 computes the argon line radiation to occur during the pinch phase reaching a value of 0.17 J emitted from the pinch.

VI. CONCLUSION

A model and code for the theta pinch has been developed and the results are consistent with the current, trajectory, and temperature measurements of the Chulalongkorn PICP experiment. From the computed and experimental results, it is clear that the Chulalongkorn theta pinch is not efficiently coupled to the primary loop current. The main inefficiency is the current coupling coefficient which is only 0.2 resulting in an argon line yield of 0.17 J (Fig. 9) or 0.01% of storage energy. The poor coupling is likely due to the low speed of the radial inward shock waves resulting in low magnetic Reynolds numbers associated with the electromagnetic drive.[23,24] With higher shock speeds, this coupling coefficient could be improved to the 0.5 level and the plasma would be more efficiently heated throughout the theta pinch phases. The code could be used to estimate what the improved plasma conditions could be.

For example, changing the value of f to 0.5 increases the on-axis shock speed to 4.6 cm/μs, pinch temperature to 150 000 K and Z to 6 with an increased argon line yield of 0.9 J. Increasing the charging voltage to 15 kV and operating at a higher pressure of 0.1 Torr, the pinch temperature is increased further to 215 000 K with a Z of 7.2 and argon line yield of 35 J or 0.5% of storage energy. Strong radiative cooling effects are observed in the results of the numerical experiments at 15 kV. A reduction in operating pressure would further increase the pinch temperature to reach a closed sub-shell Z value of 8. Numerical experiments on other gases, such as neon krypton and xenon, could also be run to extend the range of the work. Depending on the intended use of the plasma, the density and temperature in various gases may be adjusted accordingly, using the code as a guide.

ACKNOWLEDGMENTS

S. Lee acknowledges a grant from Chulalongkorn University for a lecture visit in July 2004, which resulted in this code being developed for the Chulalongkorn PICP. We acknowledge that parts of this code had been used in a published paper.[1] S.L. acknowledges UM.S/625/3/HIR/43 and UMRG102/10AFR and S.H.S. acknowledges research Grant Nos. INT-CPR-01-02-2012 and FRGS/2/2013/SG02/INTI/01/1 in the preparation of this paper.

[1]S. Chaisombata, D. Ngamrungroj, P. Tangjitsomboon, and R. Mongkolnavin, Procedia Eng. **32**, 929–935 (2012).
[2]F. R. T. Luna, G. H. Cavalcanti, and A. G. Trigueiros, J. Phys. D: Appl. Phys. **31**(7), 866 (1998).
[3]S. Lee, Radiative Dense Plasma Focus Computation Package: RADPF, 2014, see http://www.plasmafocus.net; http://www.intimal.edu.my/school/fas/UFLF/ (archival websites).
[4]S. Lee, "Plasma focus radiative model: Review of the Lee model code," J. Fusion Energy **33**, 319–335 (2014).
[5]D. E. Potter, Nucl. Fusion **18**, 813–823 (1978).
[6]M. Krishnan, IEEE Trans. Plasma Sci. **40**(12), 3189–3221 (2012).
[7]A. E. Robson, Phys. Fluid **B3**, 1481 (1991).
[8]See http://www.plasmafocus.net/IPFS/modelpackage/File3Appendix.pdf for NAD Khattak, anomalous Heating (LHDI), 2011.
[9]S. Lee, "Radiation in Plasmas," in *Proceedings of Spring College in Plasma Physics, ICTP, Trieste, 1983*, edited by B. McNamara (World Scientific Publishing Company, Singapore, 1984), Vol. II, pp. 978–987.
[10]S. Lee and A. Serban, IEEE Trans. Plasma Sci. **24**, 1101–1105 (1996).
[11]"Laser and plasma technology," in *Proceedings of First Tropical College on Applied Physics, 26 December 1983-14 January 1984*, edited by S. Lee, B. C. Tan, C. S. Wong, and A. C. Chew (World Scientific Publishing Company, Singapore, 1985), pp. 38–62.
[12]R. A. Gross, Rev. Mod. Phys. **37**, 724–743 (1965).
[13]L. Spitzer, *Physics of Fully Ionised Gases*, Interscience Tracts on Physics and Astronomy (Interscience, New York, 1965).
[14]J. W. Shearer, Phys. Fluids **19**, 1426 (1976).
[15]R. Pease, Proc. Phys. Soc. **70**, 11 (1957).
[16]S. Braginskii, Zh. Eksp. Teor. Fiz. **33**, 645 (1957).
[17]K. Koshelev and N. Pereira, J. Appl. Phys. **69**, 21–44 (1991).
[18]S. Lee, S. H. Saw, and J. Ali, J. Fusion Energy **32**, 42–49 (2013).
[19]See www.plasmafocus.net/IPFS/modelpackage/Corona%20Calculations/C1coronaIntroduction.htm for the code for calculating the effective charge and specific heat ratio as functions of temperature.
[20]S. Lee, Aust. J. Phys. **36**, 891–895 (1983).
[21]E. B. Saloman, J. Phys. Chem. Ref. Data **39**(3), 033101 (2010).
[22]See http://www.nist.gov/pml/data/asd.cfm for NIST.
[23]S. Lee, M. Eissa, A. V. Gholap, K. H. Kwek, S. Mulyodrono, S. Sapru, A. J. Smith, T. Y. Suryadi, W. Tou, C. S. Wong, W. Usada, and M. Zakaullah, Singapore J. Phys. **3**, 75–82 (1986).
[24]S. Lee, S. H. Saw, P. C. K. Lee, R. S. Rawat, and K. Devi, J. Fusion Energy **32**, 50–55 (2013).